Convective Diffusion of Heat in Composite Media with Heat Sources and Sinks

B. S. BAKER, DIMITRI GIDASPOW

Institute of Gas Technology, Chicago, Illinois

and **D. T. WASAN**

Illinois Institute of Technology, Chicago, Illinois

Convective diffusion of heat is a problem which arises in many areas. Since most thermal transport situations involve more than one material insulation, supports, etc., the treatment of composite regions is of interest. In certain systems, namely, those involving chemical or nuclear reactions, heat generation may be either localized or distributed. In this paper a general analytical treatment of this problem is made by using a double Fourier series technique involving an extended orthogonality concept. This treatment is then applied to the solutions of heat transfer situations arising in electrochemical energy conversion systems. Experimental temperature profiles are presented which test the theory.

Early work (*1, 2*) on heat transfer in electrochemical energy conversion systems treated the multidimensional unsteady problem of temperature distribution in a stack in which heat is generated by means of the irreversibility associated with the electrochemical process. In this paper we will extend the analysis to include cell geometries where both heat-generating and heat-adsorbing reactions take place at the same time but in different locations within the cell. This latter situation arises if a hydrocarbon is being reformed into hydrogen and carbon dioxide. Further treatment of the insulated cell will also be considered since the above phenomena usually takes place in elevated temperature systems which in practice are insulated from surroundings.

The source-sink portion of the problem will be handled by use of a double Fourier series technique. The composite-region part of the problem arising from the insulated cell geometry will be treated by means of an extended orthogonality concept. Finally, the theory will be compared with experiment by using a Green's function derived (3) version of the solution.

MATHEMATICAL MODEL

A fuel cell stack consists of a multiplicity of single cells. For a many-celled stack it is possible to consider a single element to be two-dimensional, that is, that there is no heat transfer in the direction of stacking. In the most general terms the resulting single two-dimensional cell is made up of a number of individual elements, electrodes, electrolytes, etc., which for the purpose of analysis can be represented by a single average thermal conductivity.

Within the plane of the electrodes of the cell it is possible to identify three distinct regions. (A typical cell with these regions is shown in Figure 1.) The first region is that occupied by the electrodes and is the electrochemically active portion of the cell and is a region of heat evolution. The second region, if it exists at all, will be that region occupied by, say, a reforming catalyst. This region may coincide with all or part of the electrode region and represents a heat sink since the reforming reaction is endothermic. The final region is a peripheral one where there is no heat generation or absorption, and this corresponds to the flanges of the cell.

As indicated in Figure 1 a gas flow takes place over the surface of the cell corresponding mainly to the flow of oxidant, air. This flow is essentially one-dimensional achieved by means of a distributor. Finally there is a region adjacent to the fuel cell through which gas flows which represents the insulation. The cell is insulated both at the gas inlet and the gas outlet ends of the cell but for numerical simplicity only the case of the double-composite region will be considered in detail in this paper, although the solution to the triple-region problem has been worked out in detail (*4*). The cell is also insulated in the direction normal to gas flow but the effect of insulation in this region will, like the exit region, be accounted for by a fictitious Biot number.

The steady state problem represented by this geometry can be described by the following equations in terms of the temperature difference:

Region 1 (The fuel cell)

$$\nabla^2 T_1 - N_{Pe_1} \frac{\partial T_1}{\partial y} = -\psi_1 \qquad (1)$$

Region 2 (The insulation)

$$\nabla^2 T_2 - N_{Pe_2} \frac{\partial T_2}{\partial y} = -\psi_2 \qquad (2)$$

The boundary conditions can be written as

$$\text{at} \quad x = 0, \quad \frac{\partial T_1}{\partial x} = \frac{\partial T_2}{\partial x} = 0, \quad -1 \leq y \leq 1 \qquad (3)$$

M. B. Baker is with Energy Research Corp., Bethel, Conn.

by symmetry

$$\text{at} \quad x = 1/2, \quad -\frac{\partial T_1}{\partial x} = N_{Bi_1} T_1, \quad 0 \leq y \leq 1 \qquad (4)$$

and

$$-\frac{\partial T_2}{\partial x} = N_{Bi_1} T_2, \quad -1 \leq y \leq 0 \qquad (5)$$

using the fictitious Biot number concept

$$\text{at} \quad y = 1, \quad -\frac{\partial T_1}{\partial y} = N_{Bi_1} T_1 \qquad (6)$$

again using the Biot number concept

$$\text{at} \quad y = -1, \quad \frac{\partial T_2}{\partial y} = (N_{Bi_2} + N_{Pe_2})\, T_2 \qquad (7)$$

by energy balance at the inlet face

$$\text{at} \quad y = 0, \quad K_2 \frac{\partial T_2}{\partial y} = K_1 \frac{\partial T_1}{\partial y} \text{ and } T_1 = T_2 \qquad (8)$$

due to equality of fluxes and continuity of temperatures at the interface.

Boundary condition (3) simply expresses the cell symmetry about a center line in the direction of gas flow. Conditions (4), (5), and (6) are the convection conditions that would be normally encountered in real systems. Condition (7) represents convection but also accounts for the fact that energy can enter the system with the inlet gas. Condition (8) expresses the constant temperature and fluxes which must exist at the junction between fuel cell and insulation.

In boundary condition (5) it has been assumed that the effective Biot numbers for the insulation region and fuel cell region are the same. This is not true. However, by using the effective Biot number of the fuel cell region we have in effect added insulation to the x direction in region 2, and it is reasonable on physical grounds that this situation will not materially affect the temperature distribution in the fuel cell. This restriction will at a later point be removed.

The system of Equations (1) through (8) describes the geometry and physical situation given in Figure 1. The solution to this set of equations is set forth below.

SOLUTION

The Double Fourier Series Method

The problem described above can be most readily handled as a dual eigenvalue problem. By addressing ourselves to the homogeneous problem of no heat generation in both regions, it is possible to find a solution to the problem by means of separation of variables. This solution is given by

$$T_1 = e^{N_{Pe_1} y/2} \sum_m \sum_n A_{m,n} \cos \lambda_m \left(\Gamma_{1_n} \sin a_n y + \cos a_n y\right)$$

$$T_2 = e^{N_{Pe_2} y/2} \sum_m \sum_n A'_{m,n} \cos \lambda_m x \left(\Gamma_{2_n} \sin a_n y + \cos a_n y\right) \qquad (9)$$

where

$$\Gamma_{1_n} = \frac{a_n \sin a_n - \sigma_1 \cos a_n}{a_n \cos a_n + \sigma_1 \sin a_n}$$

$$\Gamma_{2_n} = \frac{\sigma_2 \cos a_n - a_n \sin a_n}{a_n \cos a_n + \sigma_2 \sin a_n}$$

for regions 1 and 2, respectively, and a_n is defined by

$$a_n^2 \equiv \gamma_n^2 - \frac{N^2_{Pe}}{4}$$

γ_n^2 being the separation of variables constant for the y direction and is determined from the frequency equation

$$K_1 \Gamma_{1_n} = K_2 \Gamma_{2_n}$$

λ_m, the eigenvalues defined for the x direction, is given by the more common frequency equation

$$\lambda_m \tan \frac{\lambda_m}{2} = N_{Bi_1}$$

The orthogonality constant $A_{m,n}$ cannot be found in the usual fashion for this problem since boundary condition (8) is not a Sturm-Liouville condition. It is necessary therefore to extend the orthogonality concept (5). To do this we must derive a new orthogonality condition for boundary condition (8).

The technique requires the equations derived by the method of separation of variables to be put into a Sturm-Liouville form by selection of the proper integrating factor. In this problem both regions must be used simultaneously. The resulting new orthogonality conditions are for the y direction

$$\int_0^1 Y_{1i}\, Y_{1j}\, e^{-N_{Pe_1} y}\, K_1\, A_{m,i}\, A_{m,j}\, dy + \int_{-1}^0 Y_{2i}\, Y_{2j}\, K_2\, A'_{m,i}\, A'_{m,j}\, e^{-N_{Pe_2} y}\, dy = 0 \qquad (10)$$

and for the x direction

$$\int_0^{1/2} A_{r,n}\, A_{s,n}\, X_r X_s\, dx = 0 \qquad (11)$$

If we now substitute expression (9) for T_1 and T_2 back into Equations (1) and (2) and use the extended orthogonality condition given by (10), and the conventional orthogonality condition given by (11), and let $m = r = s$ and $n = i = j$, we get, solving for $A_{m,n}$

$$A_{m,n} = \frac{K_1 \int_{①}\int \psi_1\, e^{-N_{Pe_1} y/2} \cos \lambda_m x \left[\Gamma_{1_n} \sin a_n y + \cos a_n y\right] dx dy + K_2 \int_{②}\int \psi_2\, e^{-N_{Pe_2} y/2} \cos \lambda_m x \left[\Gamma_{2_n} \sin a_n y + \cos a_n y\right] dx dy}{{}_1\alpha_{m,n}\, K_1 \int_0^1 \int_0^{1/2} \cos^2 \lambda_m x \left[\Gamma_{1_n} \sin a_n y + \cos a_n y\right]^2 dx dy + {}_2\alpha_{m,n}\, K_2 \int_{-1}^0 \int_0^{1/2} \cos^2 \lambda_m x \left[\Gamma_{2_n} \sin a_n y + \cos a_n y\right]^2 dx dy} \qquad (12)$$

where

$${}_1\alpha_{m,n} \equiv \lambda^2_m + a^2_n + \frac{N^2_{Pe_1}}{4} \quad \text{and}$$

$${}_2\alpha_{m,n} \equiv \lambda^2_m + a^2_n + \frac{N^2_{Pe_2}}{4}$$

Equation (12) along with Equation (9) give the complete description of the temperature field. It should be noted that for this particular problem there is no heat generation in the insulation, and (12) can be somewhat simplified by letting $\psi_2 = 0$. To explain the problem fully some interpretation of the remaining integral in the numerator of Equation (12) is required.

Source-Sink Zones and the Definition of $\int_{①}\int$

The zone of integration represented by the double in-

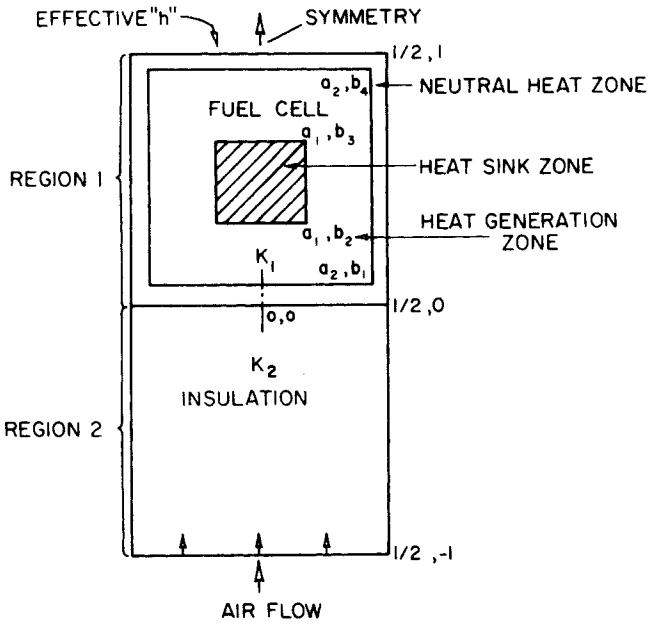

Fig. 1. Mathematical representation of two-dimensional cell showing fuel cell reforming heat active region 1 and the insulation heat passive region 2.

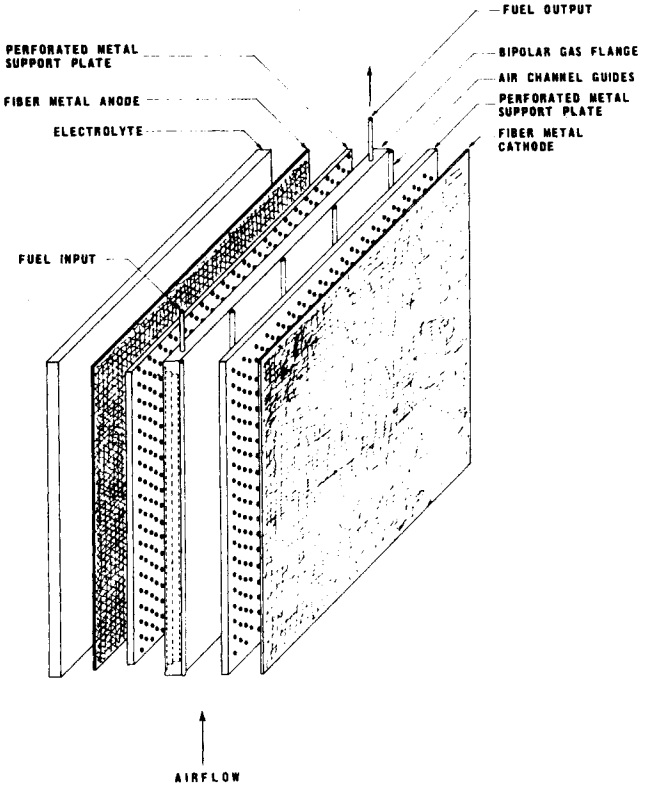

Fig. 2. Basic cell design showing how real cell components are stacked.

tegral $\int_{①}\int$ in the numerator of (12) represents the total area of region 1 over which heat is either generated or absorbed.

In the evaluation of $A_{m,n}$ in the present problem where ψ_2 is equal to zero we focus attention on the quantity

$$N_{n,m} \equiv K_1 \int_{①}\int \psi_1 \, e^{-N_{Pe_1} y/2} \cos \lambda_m x \, [\Gamma_{1n} \sin a_n y + \cos a_n y] \, dx \, dy \quad (13)$$

ψ_1 takes on different values in region 1. Referring to Figure 1 we see that around the edge of the cell corresponding to the inert flange there is no heat generation; therefore the contribution of this section to the value of $N_{n,m}$ is zero. In the interior regions there are two distinct heat zones. The simplest heat zone is that in which heat is generated by processes associated with cell irreversibility. The extent of this heat generation is given by

$$\psi = \frac{I^2 IN}{K} \left[\left(3.413a - \frac{T\Delta S}{nF} + 3.413I \, (b + ps) \right) \right] \quad (14)$$

In the second heat zone there can be either heat generation or absorption since both electrochemical and chemical reactions are taking place in this area. If we let ψ^* represent the extent of reforming taking place in the zone, then

$$\psi^* = \frac{\Delta H_R F_S N}{K} \quad (15)$$

Equations (14) and (15) can be combined to give ψ', the heat quantity which describes this source-sink region:

$$\psi' = \left(\psi - \frac{1}{A_f} \psi^* \right) \quad (16)$$

Now aided by Figure 1 it is possible to define quantitatively the zone of heat generation given by (13).

$$N_{n,m} = \left[\int_0^{a_2} \int_{b_1}^{b_2} \psi + \int_{a_1}^{a_2} \int_{b_2}^{b_3} \psi + \int_0^{a_2} \int_{b_3}^{b_4} \psi \right]$$

$$\cos \lambda_m x \, (\Gamma_{1n} \sin a_n y + \cos a_n y) e^{-N_{Pe_1} y/2} \, dx dy$$

$$+ \int_0^{a_1} \int_{b_2}^{b_3} \psi' \cos \lambda_m x (\Gamma_{1n} \sin a_n y + \cos a_n y) e^{-N_{Pe_1} y/2} \, dx dy \quad (17)$$

Equation (17) illustrates how the geometry of the heat generation field participates in the problem. Using this double series method, developed originally for the treatment of problems in electromagnetic theory (6), it is possible to readily change the location of sources and sinks simply by changing the limits of integration in Equation (17). Thus, having solved the problem for a single geometry, one can use Equation (17) as a handy design tool. The complete solution to the temperature distribution within the fuel cell is given by Equations (9), (12), (16), and (17) can be written as

$$T_1 = e^{-N_{Pe_1} y/2} \sum_m \sum_n \frac{N_{n,m}}{D_{n,m}} \cos \lambda_m x (\Gamma_{1n} \sin a_n y + \cos a_n y) \quad (18)$$

where $D_{n,m}$ is the denominator of Equation (12).

Temperature Profile Solutions by the Method of Green's Functions

The temperature field given by Equation (18) is dependent on having a good estimate of a Biot number at $x = 1/2$ and the assumption leading to equal λ eigenvalues previously discussed. A more accurate and more easily experimentally verifiable problem would involve the knowledge of a measured temperature profile at the x extremity. If we replace the convection boundary condition given by Equations (4) and (5) with the new condition

$$\text{at} \quad x = 1/2, \quad T = T(y), \quad -1 \leq y \leq 1 \quad (19)$$

we give rise to a nonhomogeneous problem closely related

(18) prior to integration as

$$G = \frac{e^{N_{Pe_1}(y-y')/2} \sum_n \sum_m K_1 \cos \lambda_m x \cos \lambda_m x' (\Gamma_{1_n} \sin a_n y + \cos a_n y)(\Gamma_{1_n} \sin a_n y' + \cos a_n y')}{D_{n,m}}$$

$$+ \frac{e^{\frac{1}{2}(N_{Pe_1} y - N_{Pe_2} y')} \sum_n \sum_m K_2 \cos \lambda_m x \cos \lambda_m x' (\Gamma_{2_n} \sin a_n y + \cos a_n y)(\Gamma_{2_n} \sin a_n y' + \cos a_n y')}{D_{n,m}} \quad (21)$$

Substitution of (21) into (20) yields

$$T_1(x, y) = e^{N_{Pe_1} y/2} \frac{\sum \sum \cos \lambda^*_m x (\Gamma_{1_n} \sin a_n y + \cos a_n y)}{D_{n,m}} \cdot N_{n,m}(x, y)$$

$$+ \frac{e^{N_{Pe_1} y/2} \sum_m \sum_n K_1 \int_0^1 T(y') \lambda^*_m \sin \frac{\lambda^*_m}{2} (\Gamma_{1_n} \sin a_n y' + \cos a_n y') e^{\frac{-N_{Pe_1} y'}{2}} dy'}{D_{n,m}}$$

$$+ \frac{e^{N_{Pe_1} y/2} \sum_m \sum_n K_2 \int_{-1}^0 T(y') \lambda^*_m \sin \frac{\lambda^*_m}{2} (\Gamma_{2_n} \sin a_n y' + \cos a_n y') e^{\frac{-N_{Pe_2} y'}{2}} dy'}{D_{n,m}} \quad (22)$$

to the previous one. The solution to this new problem is readily obtained from the other solution by the method outlined by Gidaspow (3) employing the Green's function concept. The solution to the new problem can be written as

$$T_1(x, y) = \iint \psi G(x, y; x', y') dx' dy' - \oint T(y') \frac{\partial G}{\partial n'} (x, y, x's y's) dy' \quad (20)$$

where G is the Green's function for the homogeneous problem corresponding to $T(y) = 0$ at $x = 1/2$. The Green's function itself has already been found in the course of solving the earlier problem and can be obtained from where the line integral corresponding to the second term on the right-hand side of (20) is evaluated along the nonhomogeneous boundary $T(y')$ and is everywhere else equal to zero by construction. The λ^*_m indicates the new eigenvalue corresponding to the $T = 0$ condition of the new homogeneous problem for which the Green's function is defined. These new eigenvalues take on the values $(2m + 1)\pi$. Equation (22) is most convenient. It permits an experimentally determined temperature profile $T(y')$ to be used as a boundary condition for predicting internal fuel cell temperatures.

Examination of Equation (21) suggests that the Green's function G can be written as

$$G \doteq G_{11} + G_{12} \quad (23)$$

Equation (23) can be interpreted as follows. G_{11} represents the temperature field in the fuel cell due to itself and G_{12} is the temperature field in the fuel cell due to the temperature distribution in the insulation. The same general form appears with three terms for the three-region problem (4). This solution can also be extended to some n region problems and to the three-dimensional situation using triple Fourier series.

The general result given by (22) was next compared with experimental data.

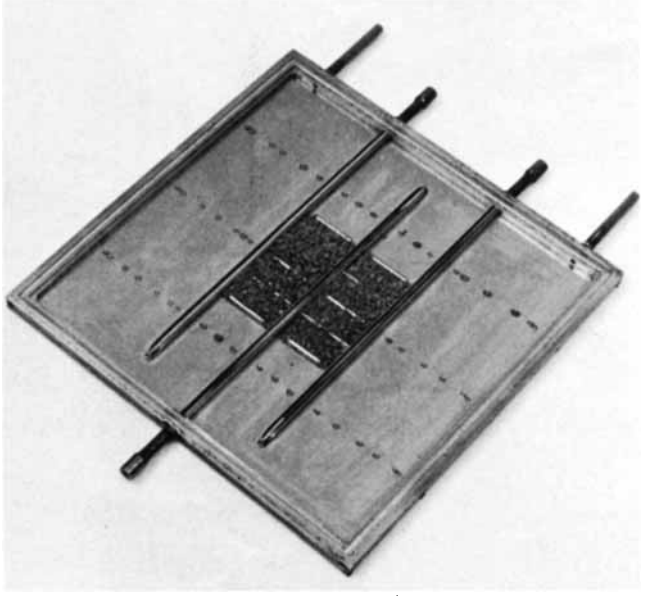

Fig. 3. Anode chamber showing location of chemical and electrochemically active heat zones with region 1 of Figure 1.

EXPERIMENTAL PROCEDURE

An experiment was designed to test the above theory. A high temperature molten carbonate fuel cell was designed, constructed, instrumented; and operated. The experiment allowed temperature distribution to be determined in a cell in which both electrochemical and reforming reactions could take place. The basic cell design employed is shown schematically in Figure 2, and the interior section of the anode chamber showing the disposition of reforming catalyst is shown in Figure 3. Figures 2 and 3 were translated into a mathematical geometry in Figure 1.

The fuel cell consists of a fiber metal nickel anode and copper cathode, the latter existing as copper oxide in actual cell operation. The electrolyte for the cell is a mixture of lithium (27% weight), sodium (41%), and potassium carbonates (32%) contained in a magnesium oxide matrix (60% total weight). Details of this type cell have been presented

TABLE 1. EXPERIMENTAL DATA

Run No.	Fuel	ψ	ψ'	N_{Pe1}	N_{Pe2}
1	H_2	214	214	0.115	2.33
2	H_2	360	360	0.204	4.13
3	H_2	360	360	0.215	4.35
6	H_2	360	360	0.138	2.8
7	CH_4	360	−94	0.138	2.8
8	CH_4	360	−450	0.138	2.8

elsewhere (7, 8).

To achieve a reasonable facsimile of a two-dimensional fuel cell geometry, a five-cell stack was constructed. The temperature field was measured at 50 points within the third or middle cell of the stack. Compensating heaters were placed adjacent to the first and fifth cells at the end of the stack to ensure an adiabatic middle cell. It is estimated that heat gains or losses of less than 5% were experienced in the middle cell in the direction of stacking as a result of its symmetrical location and the compensating heaters. Adiabaticity of the third cell in the direction of stacking was determined by measuring the temperature field in the second and fourth cells of the stack and comparing local temperature gradients in the direction of stacking.

The fuel used in the experiments was a hydrogen-nitrogen-water or hydrogen-methane-nitrogen-water mixture (for the reforming tests). The oxidant was a mixture of carbon dioxide and oxygen. Oxidant flows were substantially greater than fuel flows and the Peclet number is based entirely on oxidant flow.

Characteristic parameters N_{Pe}, N_{Bi} have been based on a value of thermal conductivity arrived at by estimating the contribution of each component of Figure 2. The value used was $K = 2.2$ B.t.u./(hr.)(ft.)(°F.).

The heat generation parameters ψ and ψ' were estimated from the experimental voltage-current curves, gas flow rates, gas composition, and geometry of electrode and reforming catalyst locations.

A detailed description of the fuel cell, experimental apparatus, instrumentation, and parameter estimation is given elsewhere (4).

RESULTS AND DISCUSSION

The experiments were devised to compare directly the theoretical and observed temperature distributions and to examine the effects of characteristic parameters, such as the Peclet and Biot numbers and heat sources. In the original work (4) comparisons were made between both single- and composite-region problem theory and experimental data, but since only the composite-region problem was described here the discussion will be limited to that area.

As shown in the earlier work (1) both convection and conduction are important. At the low values of Peclet number (for example, 0.2) which characterize these experiments, conduction is the dominant mode of heat transfer. It is possible that conditions could arise where cathodic gas flows would be increased giving rise to a Peclet number of about 2, but it is unlikely that higher values could be employed in practical systems. Hence both conduction and convection will always be important. Because this work is characterized by low Peclet numbers and conduction is dominant, it is important to examine the coupled two-region problem where abrupt conductivity changes take place between the insulation and the fuel cell.

An experimental temperature profile $T(y)$ was determined by measuring 12 point temperatures at the x extremity of the fuel cell and insulation. These data were then fitted numerically by a least squares quadratic function in the fuel cell region and by a 10-segment linearization of the data in the insulation region.

A summary of pertinent experimental data is given in Table 1. Certain tests conducted for the purpose of duplication and checking are deleted from the original results.

In Figure 4 a comparison is shown between theoretical and experimental temperature distributions. The particular data shown are for the temperature distribution at the center of the cell in the direction of gas flow and are typical of agreement obtained in all runs.

A further comparison between experiment and theory is shown in Figure 5 where the effect of flow over the range of experimental data is shown. While theory shows a somewhat stronger dependence of maximum cell temperature on the Peclet number than experiment, agreement is relatively good and the data can be fitted within a 15% variation on N_{Pe}. Additional experiments would be needed to attach significance to the slope suggested by those data points.

Of considerable practical interest is the ability to predict the effect of an internal endothermic reaction on the temperature distribution within the cell. This portion of the theory was tested by the last three experiments, and the results are shown in Figure 6. Again agreement between experiment and theory seems to have been achieved.

Based on these results it seems reasonable to say that the model presented satisfactorily describes the heat transfer phenomena in such a media.

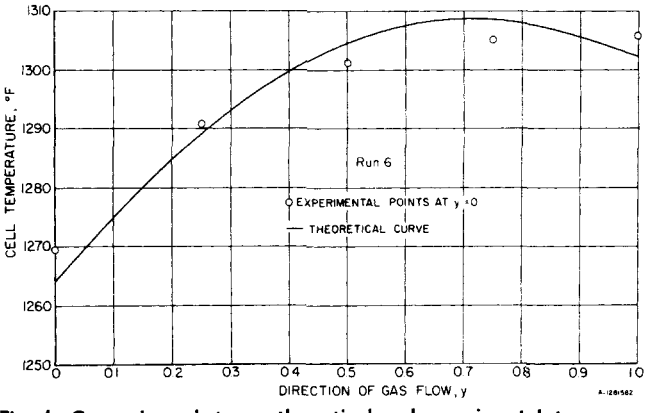

Fig. 4. Comparisons between theoretical and experimental temperature distributions within the fuel cell section (region 1) of the system.

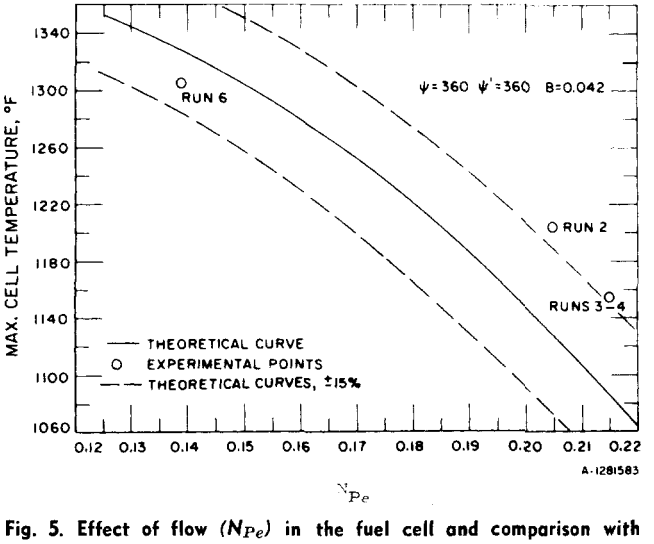

Fig. 5. Effect of flow (N_{Pe}) in the fuel cell and comparison with theory over the range experimentally investigated.

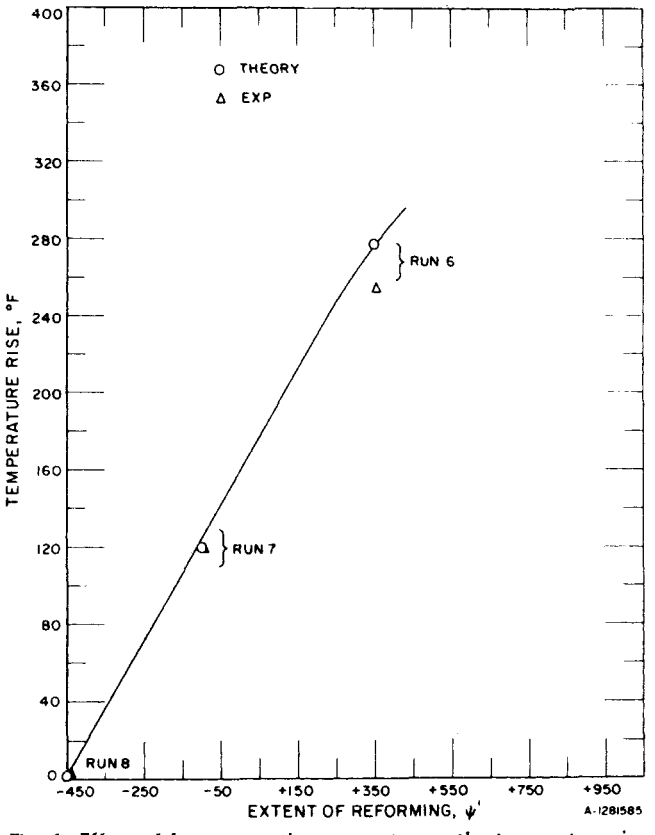

Fig. 6. Effect of heat generation parameter on the temperature rise in the cell (ψ, ψ') and comparison of theory over the range experimentally investigated.

CONCLUSIONS

The heat transfer design engineer can use the above theory to solve a variety of problems. By using the solutions obtained with homogeneous boundary value problems it is possible to predict temperature profiles within a composite solid. Physical systems wherein such phenomena exist are electrochemical cells described here, nuclear reactors where either neutron diffusion or heat flow are of interest, and chemical reaction systems with distributed reaction sites. The dual eigenvalue technique readily permits cell or reactor geometry to be changed by changing only the limits of integration to define the reaction zones. The solutions are in explicit form and converge rapidly.

The Green's function solution allows interior temperature fields to be determined by using only external thermocouple connections, thereby avoiding laborious experimental procedures.

The extended orthogonality technique permits two-dimensional composite-material problems to be solved analytically, thereby saving computation time and giving greater physical insight to the problems.

ACKNOWLEDGMENT

The authors wish to thank Lee Camara for his contributions to the experimental portion of this work and Miss Wladyslawa Toczycki who did the computer programming. The work was done as part of the Institute of Gas Technology basic research program.

NOTATION

A_f = area fraction of fuel cell occupied by the reforming catalyst
a = experimental constant defining the polarization curve [Equation (14)]
a_n = eigenvalue y direction
$a_1, a_2, b_1, b_2, b_3, b_4$ = coordinates of various zones of reaction (Figure 1)
b = experimental constant defining the polarization curve [Equation (14)]
N_{Bi} = Biot number, hl/K everywhere else
$D_{n,m}$ = denominator functions [Equation (12)]
F = Faraday constant, 12,158 (amp.)(hr.)/lb. equivalent or 96,500 coulombs/equivalent
F = hydrocarbon flow rate, lb./hr.
G = Green's function
G_{ij} = components of a Green's function matrix
ΔH_R = enthalpy function for reforming reaction
h = heat transfer coefficient at edge of fuel cell, B.t.u./(hr.)(sq.ft.)(°F.)
K = thermal conductivity, B.t.u./(hr.)(ft.)(°F.)
l = characteristic cell dimension, ft.
N = number of cells per linear foot
$N_{n,m}$ = numerator functions [Equation (17)]
N_{Pe} = Peclet number = $\rho v c_p l/K$, dimensionless
p = electrolyte resistance, ohm/cm.
s = interelectrode spacing, cm.
S = entropy function
T = temperature difference, °F. or absolute temperature when it occurs as $T\Delta S$
v = linear velocity, ft./hr.
x, y, z = reduced length coordinates in general

Greek Letters

$\alpha_{m,n}$ = see Equation (12)
λ = eigenvalue in x direction
Γ = defined by Equations (14) and (15)
$\gamma_n = \left(a_n^2 + \frac{N_{Pe}}{4}\right)^{1/2}$
ρ = density of gas, lb./cu.ft.
π = product, or 3.1416
$\sigma = N_{Bi} + N_{Pe}/2$
ψ = reduced heat generation rate, $\psi_a l^2/K = \dot{Q} N l^2/K$
ψ_a = actual rate of heat generation per unit volume, B.t.u./(hr.)(cu.ft.)
ψ' = reduced heat generation with reforming [Equation (16)]
ψ^* = heat generation in the reforming section [Equation (15)]

Subscripts

f = fuel cell
s = coordinate at a boundary
1 = fuel cell region unless otherwise stated
2 = insulation region unless otherwise stated

LITERATURE CITED

1. Gidaspow, Dimitri, and B. S. Baker, *AIChE J.*, **11**, 825 (1965).
2. ———, B. C. Jee, and F. Oliva, *Chem. Eng. Progr. Symp. Ser.*, No. 75, **63**, 63-73 (1967).
3. Gidaspow, Dimitri, *Chem. Eng. Progr. Symp. Ser.*, No. 82, **64**, 166 (1968).
4. Baker, B. S., Ph.D. thesis, Illinois Inst. Technol., Chicago (1969).
5. Sparrow, E. M., and E. C. Spalding, *J. Heat Trans.*, **90**, 115 (1968)
6. Roth, E., *Revue Generale Electricite*, **28**, 137 (1928).
7. Baker, B. S., L. G. Marianowski, J. Meek, and H. R. Linden, *Advan. Chem. Ser.*, **47**, 247 (1965).
8. Baker, B. S., L. G. Marianowski, J. Zimmer, and G. Price, in "Hydrocarbon Fuel Cell Technology," B. S. Baker, ed., p. 293, Academic Press, New York (1965).

Manuscript received June 9, 1969; revision received November 6, 1969; paper accepted November 10, 1969.